



# Corrosion behavior of steels in flowing lead–bismuth

F. Barbier<sup>a,\*</sup>, A. Rusanov<sup>b</sup>

<sup>a</sup> CEA-CEREM/SCECF, CE Saclay, 91191 Gif-sur-Yvette cedex, France

<sup>b</sup> IPPE, Bondarenko Square 1, Obninsk, 249020, Kaluga Region, Russia

## Abstract

Corrosion of steels in a flowing Pb–Bi environment has been studied. Specimens were exposed to the melt at 300°C and 470°C for up to 3116 h. The flow velocity was close to 2 m/s and the oxygen concentration in Pb–Bi was maintained at  $1\text{--}2 \times 10^{-6}$  wt%. Independent of the specific steels (Optifer IV, T91 and EP823 martensitic steels, 1.4970 austenitic steel), no sign of dissolution was detected for either temperatures. In all cases, a protective oxide layer was formed on the steel surface. It was very thin (thickness  $\ll 1 \mu\text{m}$ ) in the case of the 1.4970 austenitic steel, which presented the maximum resistance to oxidation in Pb–Bi–O. After 3116 h at 470°C, the thickness of the oxide layer (magnetite scale  $\text{Fe}_3\text{O}_4$ ) formed on the martensitic steels ranged from about 10 to 20  $\mu\text{m}$ . The oxidation resistance of the three martensitic steels decreases in the sequence: EP823, T91 and Optifer IV. The presence of silicon in the EP823 Russian steel ( $\approx 2$  wt%) reduces the oxide layer growth. Results show that the present level of oxygen content in Pb–Bi is suitable for ensuring stable protection of steels against liquid metal corrosion at least for that period. © 2001 Elsevier Science B.V. All rights reserved.

## 1. Introduction

Accelerator driven systems (ADS) are proposed for radioactive waste transmutation [1]. They consist of an accelerator for high-energy proton generation, a spallation target to produce neutrons, and a subcritical blanket. A heavy material is preferred for the target to increase the number of spallation neutrons. In addition, liquid metal targets are of interest because heat removal and radiation damages can be more easily solved. The lead–bismuth eutectic alloy (Pb–55.2 wt% Bi) is a candidate for the target material.

Liquid metal corrosion has to be considered to select the appropriate containment material for the ADS target. This phenomenon manifests itself in various ways: dissolution, compound formation, liquid penetration at grain boundaries, etc. It is known from literature that corrosion problems arise at high temperatures when steels are in contact with a liquid lead alloy (e.g., [2–5]). The corrosion process depends on many factors: time of exposure, temperature, thermal gradient, solid and liq-

uid compositions, flow velocity, etc. In the Pb–Bi alloy, the oxygen content is a fundamental characteristic (for example, too much oxygen can lead to the oxidation of the elements exposed to the melt). The oxygen affinity of a given element is defined by the free energy of formation of the oxide, conveniently summarized as a function of temperature in the form of the well known Ellingham diagram. From this diagram, it can be shown that the oxides of Bi and Pb are less stable than the oxides that form on steels (e.g., [6]). Thus, depending on the oxygen content in the Pb–Bi alloy, the steel can be oxidized or not.

In this work, corrosion experiments have been performed in a pumped loop system with flowing Pb–Bi in the temperature range 300–470°C. Different materials (austenitic and martensitic steels) were exposed to the melt. Results are presented and discussed hereafter.

## 2. Experimental

### 2.1. Corrosion loop

The CU-1M loop of the Institute of Physics and Power Engineering was used (volume  $\approx 60$  l). It consists of a central heat exchanger, a hot section, a cold section,

\* Corresponding author. Tel.: +33-1 69 08 16 13; fax: +33-1 69 08 15 86.

E-mail address: barbier@ortolan.cea.fr (F. Barbier).

and a tank for filling and draining. Hot parts ( $T > 420^\circ\text{C}$ ) are made of 20Cr–14Ni–2Si austenitic steel, parts at lower temperature are of 18Cr–10Ni–1Ti steel. The heat exchanger is made of 13Cr–2Mo–2Si martensitic steel. A forced circulation is obtained by a centrifugal pump and the velocity is measured by an electromagnetic flowmeter. In order to maintain a constant oxygen content in Pb–Bi, the loop is equipped with a hydrogen generation system ( $\text{He}-20\% \text{H}_2$  gas) for oxygen removal and of a mass exchanger system allowing PbO dissolution for oxygen replenishment. The oxygen concentration is measured by means of an electrochemical cell (two oxygen meters are placed in the hot section).

Before filling the loop, the PbO oxides were mechanically removed from the molten Pb–Bi surface by skimming after heating the tank at  $180^\circ\text{C}$  for 48 h. In this study, it should be noted that all the steel surfaces of the loop are passivated before the Pb–Bi introduction (mainly because of previous experiments already carried out in this facility with Pb–Bi).

The operating temperature ( $T$ ) was  $470^\circ\text{C}$  in the hot test section and  $300^\circ\text{C}$  in the cold test section, the coldest point in the loop being  $250$ – $260^\circ\text{C}$ . The flow velocity was  $1.9 \pm 0.1$  m/s. The oxygen concentration in Pb–Bi ( $c_{\text{O}_2}$ ) consistently maintained at  $1$ – $2 \times 10^{-6}$  wt% during the experiments without using the systems for oxygen removal or oxygen replenishment. This was achieved thanks to the initial passivation of the surfaces of the facility.

## 2.2. Materials

The composition of the Pb–Bi alloy was (wt%): 44.42Pb–55.77Bi– $3.3 \times 10^{-4}\text{Fe}$ – $2.8 \times 10^{-3}\text{Ni}$ – $<10^{-3}\text{Cr}$ . Three martensitic steels (T91, low activation steel Optifer IVc and Russian steel EP823) and one austenitic steel (1.4970) were tested. Their chemical compositions are indicated in Table 1. Cylindrical specimens of the materials were prepared (diameter: 8 mm, length: 110 mm). No treatment was made after machining. The specimens were fixed in the hot and cold test sections of the loop. The test series of 3116 h total duration was interrupted after 1116 and 2000 h so that specimens exposed 1116, 2000 and 3116 h are available for examination.

Table 1

Chemical compositions of steels (wt%)

	Cr	Ni	Mo	Mn	V	Nb	W	Ti	Si	C
Austenitic steel 1.4970	15.4	14	1.8	2.4	–	–	–	0.4	0.5	0.12
Martensitic steel T91	8.26	0.13	0.95	0.38	0.20	0.075	–	–	0.43	0.105
Martensitic steel Optifer IVc	9.1	–	–	0.52	0.22	–	1.4	–	–	0.12
Martensitic steel EP823	12	0.89	0.7	0.67	0.43	0.4	1.2	–	1.8	0.14

## 2.3. Examination of corrosion effects

After taking the specimens out of the loop, the Pb–Bi alloy adhering on the steel surfaces was removed by immersion of the samples in glycerol at  $150$ – $180^\circ\text{C}$ . Afterwards, they were cleaned (in acetone and alcohol) and dried for visual examination and weight measurements. Finally, pieces were cut and polished for cross-section examination by optical microscopy and scanning electron microscopy (SEM). Compositional information was obtained by SEM via energy dispersive X-ray analysis (EDX) and electron microprobe analysis. In addition, X-ray diffraction was used for compound characterization.

## 3. Results and discussion

### 3.1. Weight analysis

Visual examination of specimens did not show strong liquid metal corrosion effects. However, modification of the steel surface in contact with the liquid could be detected for the martensitic steels because they were less shiny and black colored.

The weight measurements indicated no loss. Therefore, no dissolution of steel elements in the presence of Pb–Bi occurred. On the contrary, a gain of weight was measured for all the samples. The weight changes were

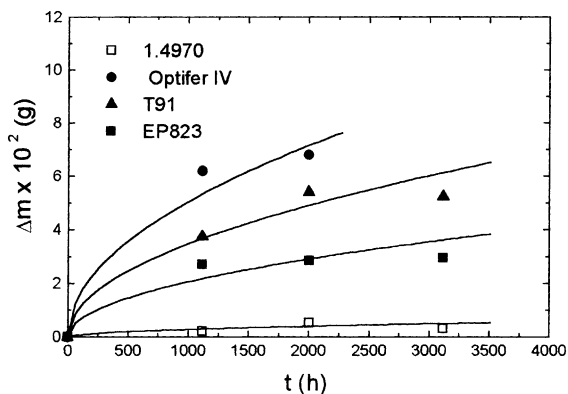


Fig. 1. Weight variation of steels exposed of flowing Pb–Bi at  $470^\circ\text{C}$  ( $c_{\text{O}_2} = 1$ – $2 \times 10^{-6}$  wt%).

extremely low at 300°C whereas they were significant at 470°C. The weight variation ( $\Delta m$ ) is related to the exposure time in Fig. 1. It is much higher for martensitic steels than for austenitic steel. The curves seem to follow a parabolic rate law (such a behavior is confirmed in Section 3.2.2).

### 3.2. Examination of the solid/liquid interface

#### 3.2.1. Austenitic steel

Whatever the temperature, no sign of corrosion damage was observed on 1.4970 steel after exposure to Pb–Bi for 3116 h. Even at 470°C (Fig. 2), this steel exhibited no Ni depletion (although nickel has a high solubility in lead alloys [7]). X-ray maps and concentration profiles obtained from the interface did not show any change in the distribution of steel elements (Fig. 3). Thus, no dissolution occurred at the interface. In fact, a very thin oxide layer (not detected by SEM, thickness

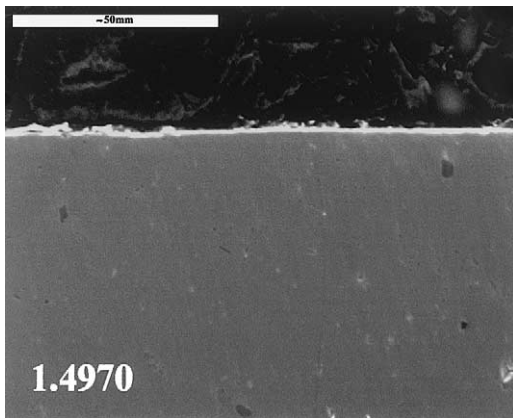


Fig. 2. Cross-section of 1.4970 austenitic steel after exposure to flowing Pb–Bi at 470°C for 3116 h ( $c_{O_2} = 1-2 \times 10^{-6}$  wt%). No corrosion damage is observed.

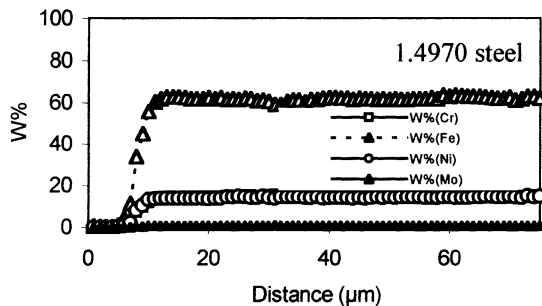


Fig. 3. Concentration profiles obtained on 1.4970 austenitic steel exposed to flowing Pb–Bi at 470°C for 3116 h ( $c_{O_2} = 1-2 \times 10^{-6}$  wt%). No Ni depletion is observed.

$\ll 1 \mu\text{m}$ ) is formed on the steel surface, providing protection against liquid metal corrosion. This is consistent with the very low gains of weight which were measured (Fig. 1).

#### 3.2.2. Martensitic steel

At 300°C, no corrosion effect was observed for the three martensitic steels exposed to Pb–Bi (Fig. 4). In some points of the surface, a corrosion product (oxide) was irregularly detected. Due to its non-uniform distri-

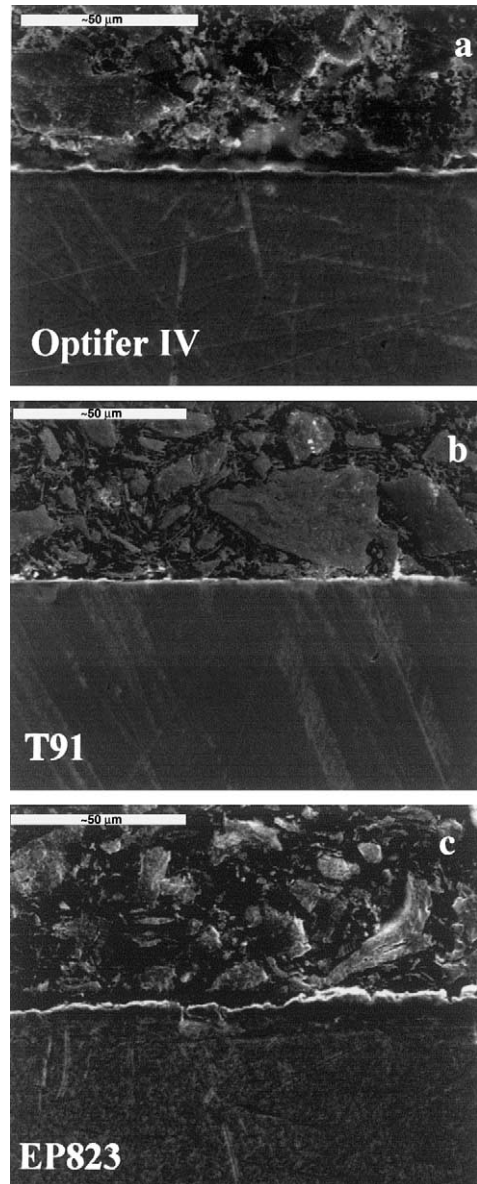


Fig. 4. Cross-sections of different martensitic steels exposed to flowing Pb–Bi at 300°C for 3116 h ( $c_{O_2} = 1-2 \times 10^{-6}$  wt%): (a) Optifer IV, (b) T91, (c) EP823.

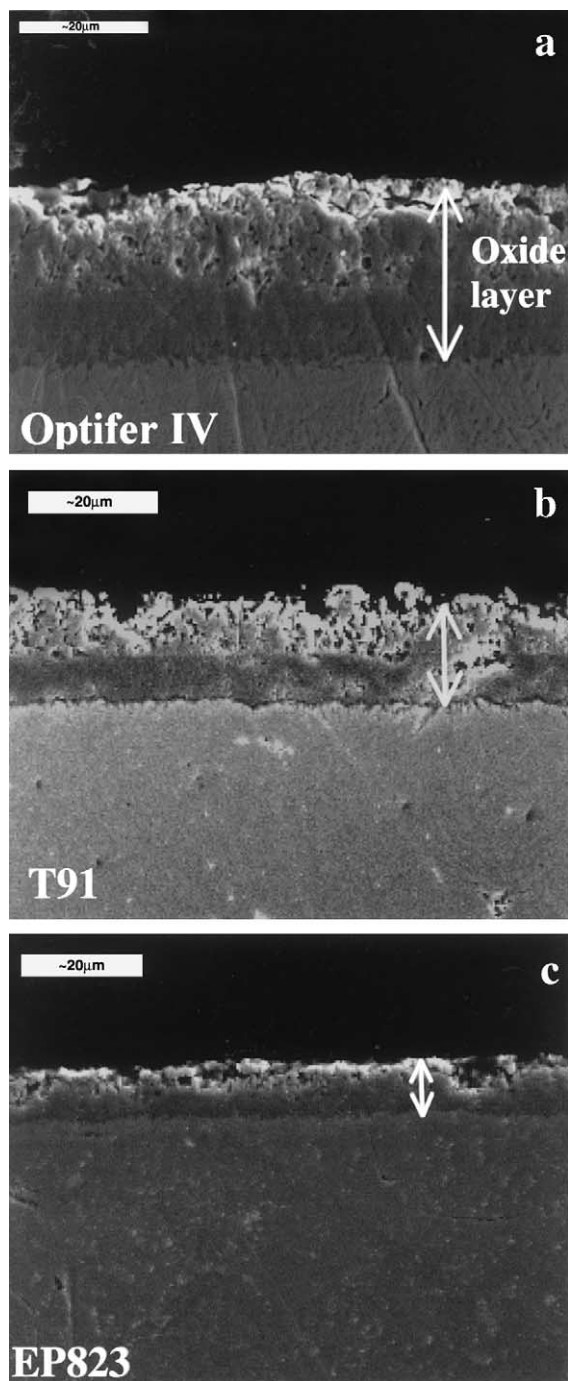


Fig. 5. Cross-sections of different martensitic steels exposed to flowing Pb–Bi at 470°C for 3116 h ( $c_{O_2} = 1-2 \times 10^{-6}$  wt%) showing the oxide layer on the surface: (a) Optifer IV, (b) T91, (c) EP823. The outer zone of the oxide layer is porous.

bution, it was not possible to evaluate its thickness. At higher temperature ( $T = 470^\circ\text{C}$ ), the behavior was quite different. The steel surface was found to be modified but

the process taking place during the solid/liquid interaction was oxidation and not dissolution. An oxide scale was clearly observed on all the steel surfaces (Fig. 5), its thickness depending on the time of exposure and the substrate (Fig. 6). The oxide formation from the oxygen present in Pb–Bi is consistent with the gain of weight observed on those materials in Fig. 1. For all martensitic steels, the growth of the oxide scale has a parabolic behavior. Depending on the steels, the oxide thickness ranges from 10 to 20 μm for the longest exposure time. It is the largest for Optifer IV steel and the smallest for EP823 steel, the T91 steel having an intermediate value. Therefore, the Russian steel EP823 has the better oxidation resistance for the conditions examined here. Such a behavior is mainly explained by the addition of silicon to this steel ( $\approx 2$  wt%). It is well established that Si added to Fe–9Cr steels reduces the oxide growth rate and thus improves the resistance to oxidation [8–10].

The oxide layer is composed of two zones: the outer part is porous whereas the inner part is compact (see for example Figs. 5(a) and (b)). In the outer zone, some parts can be spalled when the layer becomes too thick. X-ray maps and electron microprobe analyses indicate that the inner layer contains most of the alloying elements present in the steel with their weight concentrations relative to their values in the metal slightly increased: it is enriched in chromium (also in silicon in the case of EP823 steel). By contrast, the external layer has no significant alloying elements: it is practically Cr-free. The oxygen concentration in the layer is rather constant with a small increase in the external part. Concentration profiles are presented in Fig. 7. They indicate compositions (wt%) close to 70Fe–0.5Cr–27O in the external layer and 57Fe–12Cr–26O in the internal layer, which corresponds to  $\text{Fe}_3\text{O}_4$  and  $(\text{Fe}, \text{Cr})_3\text{O}_4$  compounds, respectively. Silicon (about 3.5 wt%) is also detected in the internal layer of the EP823 steel. The

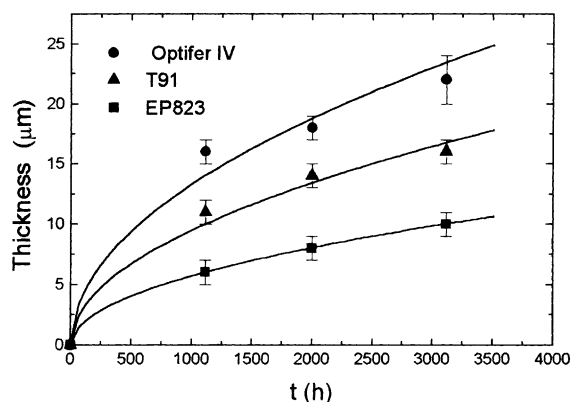


Fig. 6. Thickness variation of the total oxide layer formed on different martensitic steels exposed to flowing Pb–Bi at 470°C versus time ( $c_{O_2} = 1-2 \times 10^{-6}$  wt%).

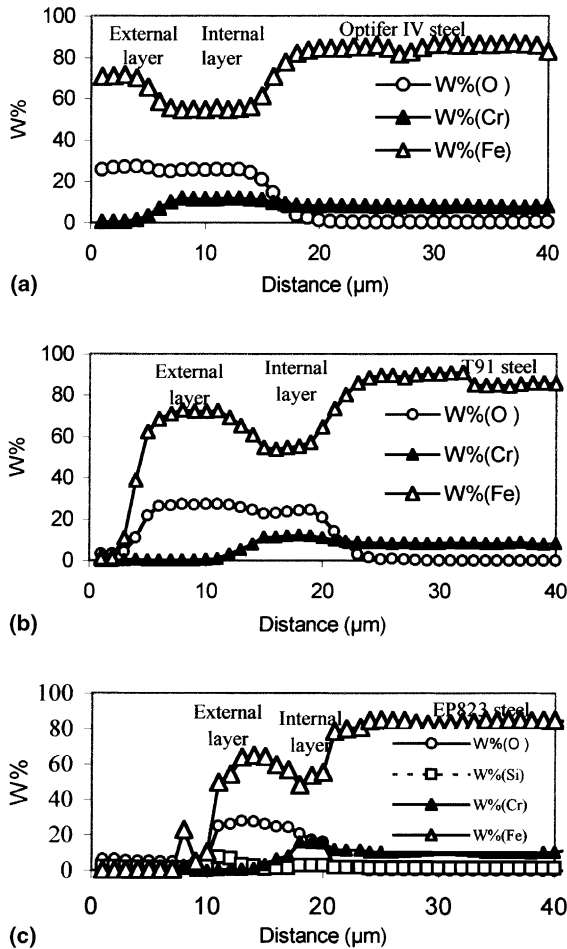


Fig. 7. Concentration profiles obtained on martensitic steels exposed to flowing Pb–Bi at 470°C for 3116 h ( $c_{O_2} = 1-2 \times 10^{-6}$  wt%): (a) Optifer IV, (b) T91, (c) EP823. The internal oxide layer is enriched in Cr, also in Si for EP823 steel (note that the Si increase also seen at the surface of the external layer is not significant: it is a polishing artifact and silicon is not detected when a solution containing alumina particles is used for final preparation of the sample).

$Fe_3O_4$  structure is confirmed by X-ray diffraction. The morphology and distribution of the elements (magnetite  $Fe_3O_4$  in the outer layer and chromium containing spinel oxide in the inner layer) are in agreement with the data reported in literature on the oxidation behavior of Fe–9Cr steels [11].

#### 4. Conclusions

At 300°C and 470°C, steels exhibited no liquid metal corrosion manifesting itself by dissolution or

intergranular liquid penetration when exposed to flowing Pb–Bi with an oxygen concentration maintained at  $1-2 \times 10^{-6}$  wt% (for a duration up to 3000 h). A protective oxide layer was formed on all steel surfaces. For 1.4970 austenitic steel, the thickness of the oxide layer is very thin but it seems sufficient to prevent preferential dissolution of nickel in the melt. For martensitic steels, the oxide layer ( $Fe_3O_4$  structure) also is effective against dissolution but its thickness is much larger, depending on the time of exposure and steel substrate. Its growth is described by a parabolic law. The 1.4970 austenitic steel has the better oxidation resistance. For martensitic steels, the resistance to oxidation decreases in the sequence: EP823, T91, Optifer IV. The presence of silicon in the EP823 Russian steel reduces the oxide growth rate, which improves the resistance to oxidation.

Results show that oxide layers formed in Pb–Bi can protect steels against dissolution in the melt. Therefore, liquid metal corrosion in liquid lead alloys can be avoided if stable protective oxide scales are formed. However, this necessitates control of the oxygen concentration in the melt. In this work, the beneficial effect of Si in the steel on the oxidation resistance is also shown. The influence of other alloying elements on the oxidation behavior of steels in Pb–Bi needs to be examined in more details. Such a study is underway on steels containing different additions of Cr, Ni, Mo, Nb, V, W, etc.

#### Acknowledgements

The authors are grateful to N. Skvortzov, Y. Pevtchich and G. Yachmenev from IPPE and F. Herbert, C. Blanc and C. Chénrière from CEA for their technical assistance in this work.

#### References

- [1] M. Salvatore, I. Slessarev, A. Zaetta, M. Delpech, G. Ritter, R. Soule, M. Vanier, CEA Report, NT-DRN-98-001, Commissariat à l'Énergie Atomique, 1998.
- [2] M. Broc, J. Sannier, G. Santarini, in: Proceedings of the BNES International Conference: Liquid Metal Engineering and Technology, BNES, London, 1984, p. 361.
- [3] J. Sannier, T. Flament, A. Terlain, Fusion Technol. 1 (1991) 901.
- [4] J. Sannier, M. Broc, T. Flament, A. Terlain, Fusion Eng. Des. 14 (1991) 299.
- [5] T. Flament, P. Tortorelli, V. Coen, H.U. Borgstedt, J. Nucl. Mater. 191–194 (1992) 132.
- [6] J. Philibert, A. Vignes, Y. Bréchet, P. Combrade, Métallurgie: du Minerai au Matériau, Masson, Paris, 1998.

- [7] M.G. Barker, T. Sample, *Fusion Eng. Des.* 14 (1991) 219.
- [8] J. Bénard, *Oxidation des Métaux*, Gauthier-Villars, Paris, 1962.
- [9] R.A. Brierley, in: *Proceedings of the BNES International Conference: Corrosion of Steels in CO<sub>2</sub>*, BNES, London, 1974, p. 165.
- [10] G.Y. Lai, *High Temperature Corrosion of Engineering Alloys*, ASM International, Materials Park, OH, 1990, p. 15.
- [11] P.C. Rowlands, D.R. Holmes, A. Whittaker, R.A. Brierley, J.C.P. Garrett, in: *Proceedings of the BNES International Conference: Gas-cooled Reactors Today*, BNES, London, 1983, p. 173.